The influence of weather regimes on European renewable energy production and demand

Karin van der Wiel[1], **Hannah C. Bloomfield**[2], **Robert W. Lee**[2,3], **Laurens P. Stoop**[4,5], **Russell Blackport**[6], **James A. Screen**[6], **Frank M. Selten**[1]

[1] Royal Netherlands Meteorological Institute, De Bilt, the Netherlands
[2] University of Reading, Department of Meteorology, Reading, United Kingdom
[3] National Centre for Atmospheric Science, Reading, United Kingdom
[4] Utrecht University, Research Institute of Informatics and Computer Science, Utrecht, the Netherlands
[5] Utrecht University, Copernicus Institute of Sustainable Development, Utrecht, the Netherlands
[6] University of Exeter, College of Engineering, Mathematics and Physical Sciences, Exeter, United Kingdom

E-mail: wiel@knmi.nl

Model Validation & Supporting Information

Two Global Climate Models (GCMs) were used in this study: EC-Earth (v2.3, Hazeleger et al., 2012) and HadGEM2-ES (Martin et al., 2011). Here we verify that these GCMs adequately reproduce the North Atlantic weather regimes, and their associated meteorological and energy surface impacts, and capture the variability within each regime. We show that the typical patterns found in the ERA5 reanalysis (Copernicus Climate Change Service, 2017), discussed in Section 3.1 of the main text, can be reproduced using GCM simulated data. Also the change in the distribution of energy variables is reproduced in the simulated data, for ERA5 data this is discussed in Section 3.2 of the main text.

These validation results give confidence in the capability of these GCMs to simulate the occurrence of extreme events within regimes in a realistic manner. It is necessary to rely on GCM simulations for the extreme event analysis, because the limited length of the reanalysis record prevents thorough investigation of extreme events, see also Section 2.1 of the main text.

1. Simulated weather regimes

As discussed in Section 2.2 of the main text, the classification of all winter days in the large ensemble simulated data was based on centroids as computed from ERA5 data. In Figure S1 the resulting circulation patterns are shown. By design of the modified classification method, the spatial patterns are very similar for the two GCMs and the ERA5. The percentage of total days assigned to each regime in the GCMs, not constrained by the method of calculation, is close to what is found for ERA5 data. The largest difference is a slight favouring of the Atlantic Ridge regime compared to ERA5. Without the spatial similarity constraints, the models still very closely reproduce the patterns computed using ERA5 data.

2. Simulated surface impacts

Figures S2 and S3 are reproductions of Figure 2 of the main text but with data from the large ensemble GCM experiments. The average surface imprints of the weather regimes on relevant meteorological variables is comparable between ERA5 and the large ensemble simulated data, though anomaly values are weaker in the EC-Earth GCM (Figure S2). Pattern correlations of GCMs versus ERA5 data, for the variables shown in these figures over a European box (15°W-35°E, 25°-70°N), range from 0.76 to 0.98. For reference a figure showing ERA-Interim data is included as well (Figure S4, pattern correlations from 0.89 to 1.00). The spatial pattern of typical renewable wind and solar energy potential in each regime (as in Figure 3 of the main text, not shown here) is also simulated well.

3. Simulated variability

In Section 3.2 we described the distribution of energy variables within each regime, Figure S5 shows the same analysis for the GCM data. Both models have a low bias in the mean energy production (Table S1), but do capture the positively skewed distributions as also found for ERA5 data (Table S3). The shift in this distribution for each of the four weather regimes is captured by both GCMs. Also the shifts in the distribution of energy demand are captured by the GCMs, though variability is lower in EC-Earth than in ERA5 and HadGEM2-ES (Table S2). Finally, the observed distribution of energy shortfall is captured by the GCMs, including the shifts corresponding to the weather regimes. Absolute model biases do not impact the analysis of extreme events in the main text, because we have based the selection of events on a model specific threshold. Though our interest here is in low production and high shortfall extremes, we note that ERA-Interim shows larger high production and low shortfall extremes than ERA5 (Figure S5a-f).

Finally, we investigate the resemblance of days classified in a regime to the regime centroid. We do so by means of a pattern correlation in the North Atlantic-European region (90°W-30°E, 20°-80°N). In Figure S6a-d it is shown that the days in a regime typically resemble the regime centroid quite well, with mean correlation coefficients of 0.48 (full range between -0.17 and 0.95). These values are systematically higher than the correlations of the days to the centroids of the other regimes (mean -0.16, range -0.93 to 0.70). Extreme events (Figure S6f-h) have comparable correlation coefficients to normal days in the regime (mean 0.53, range -0.02 to 0.88), though there seems to be a shift towards anti-correlated NAO positive patterns. We further compare anomaly magnitudes, by means of a projection of daily anomalies to the anomalies as in the regime centroid in the North Atlantic-European region, was computed for all winter days (Figure S7a-d) and for extreme events (Figure S7f-h). As for the pattern correlations, the range and mean value of the magnitudes for extreme events are comparable to those of all winter days.

4. General statistics

We include some tables of general statistical measures, computed from ERA5 and GCM simulated data. In each table the full winter value (December to February) can be compared to the value for a weather regime-subsample. Table S1 shows the mean energy production/demand/shortfall, Table S2 the standard deviations, Table S3 the skewness and finally Table S4 the risk ratios.

References

Copernicus Climate Change Service, 2017: ERA5: Fifth generation of ECMWF atmospheric reanalyses of the global climate. Copernicus Climate Change Service Climate Data Store (CDS), accessed June 2019, https://cds.climate.copernicus.eu/cdsapp#!/home.

Hazeleger, W., and Coauthors, 2012: EC-Earth V2.2: description and validation of a new seamless Earth system prediction model. *Climate dynamics*, **39 (11)**, 2611–2629, doi:10.1007/s00382-011-1228-5.

Martin, G. M., and Coauthors, 2011: The HadGEM2 family of met office unified model climate configurations. *Geoscientific Model Development*, **4 (3)**, 723–757, doi: 10.5194/gmd-4-723-2011.

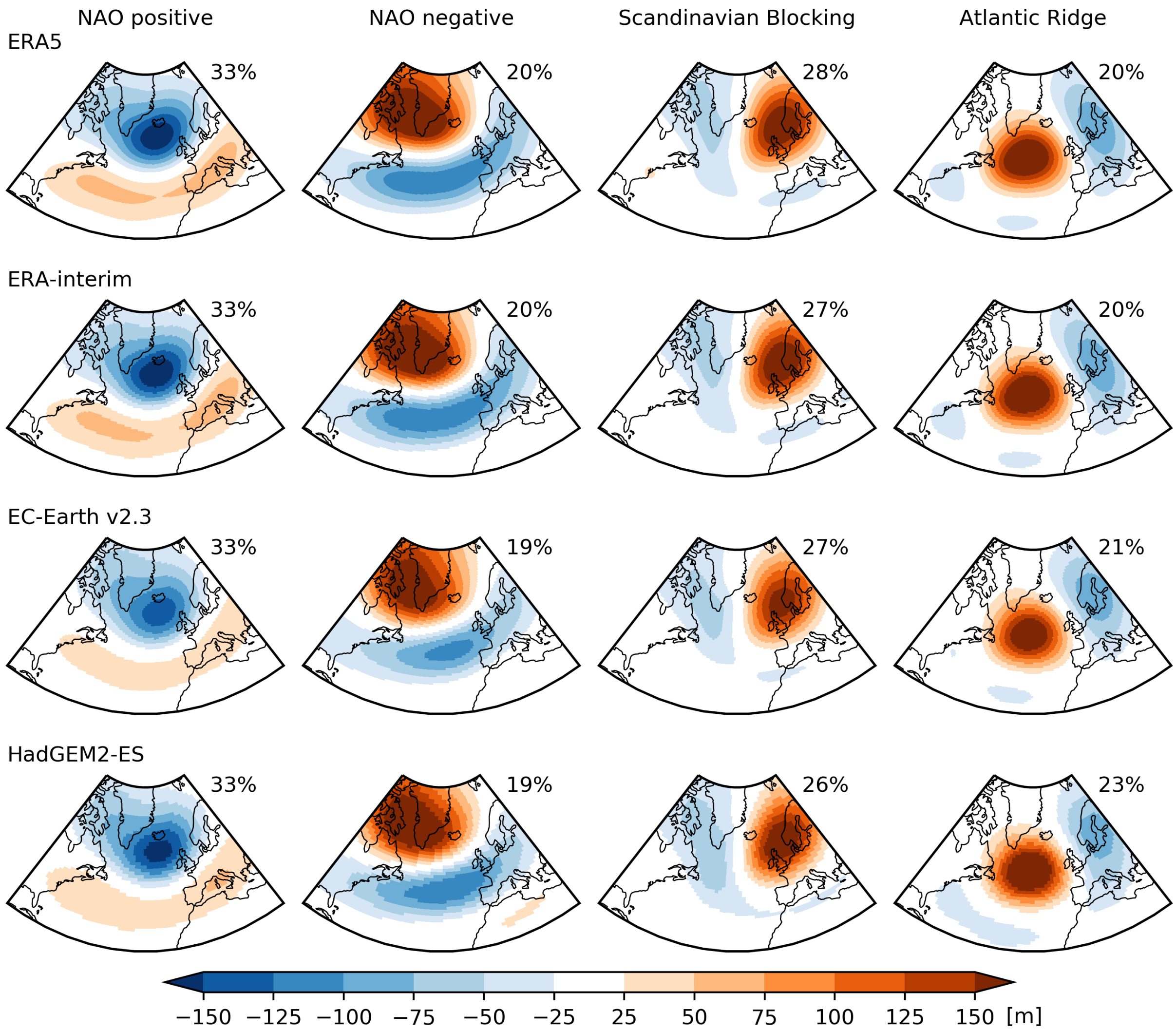

Figure S1. Four regimes of atmospheric circulation in the North Atlantic-European domain for (top) ERA5, (second row) ERA-interim, (third row) EC-Earth v2.3, (bottom) HadGEM2-ES. Colours show the 500 hPa height anomaly [m], percentage values denote the percentage of total days categorised in each regime. Classification of ERA-interim, EC-Earth and HadGEM2-ES data based pseudo-principle component time series and ERA5 centroids (see Section 2.2 of the main text).

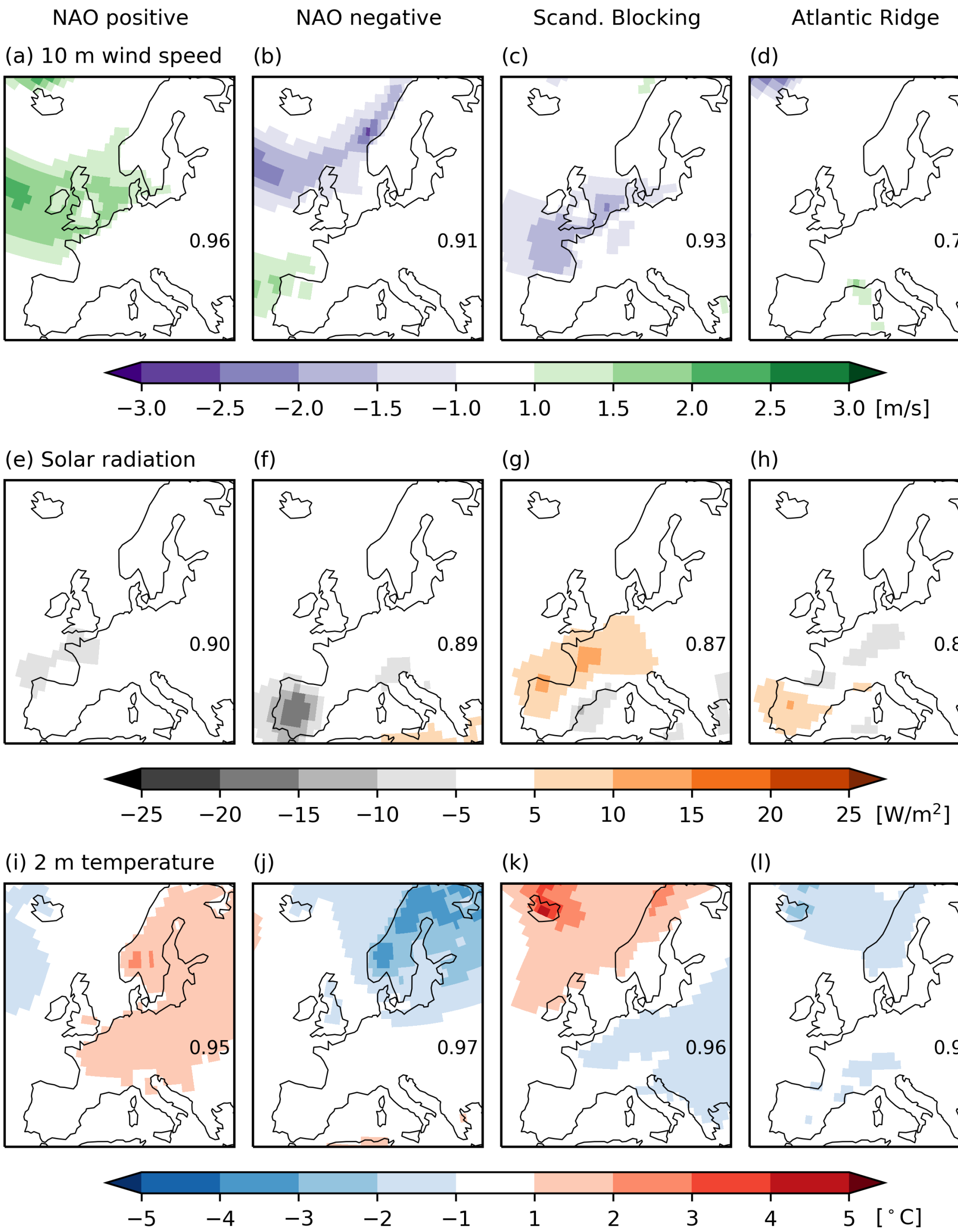

Figure S2. As Figure 2 of the main text, but here based on simulated data from the EC-Earth model. Values denote the pattern correlation coefficient between the map shown and that based on ERA5 data.

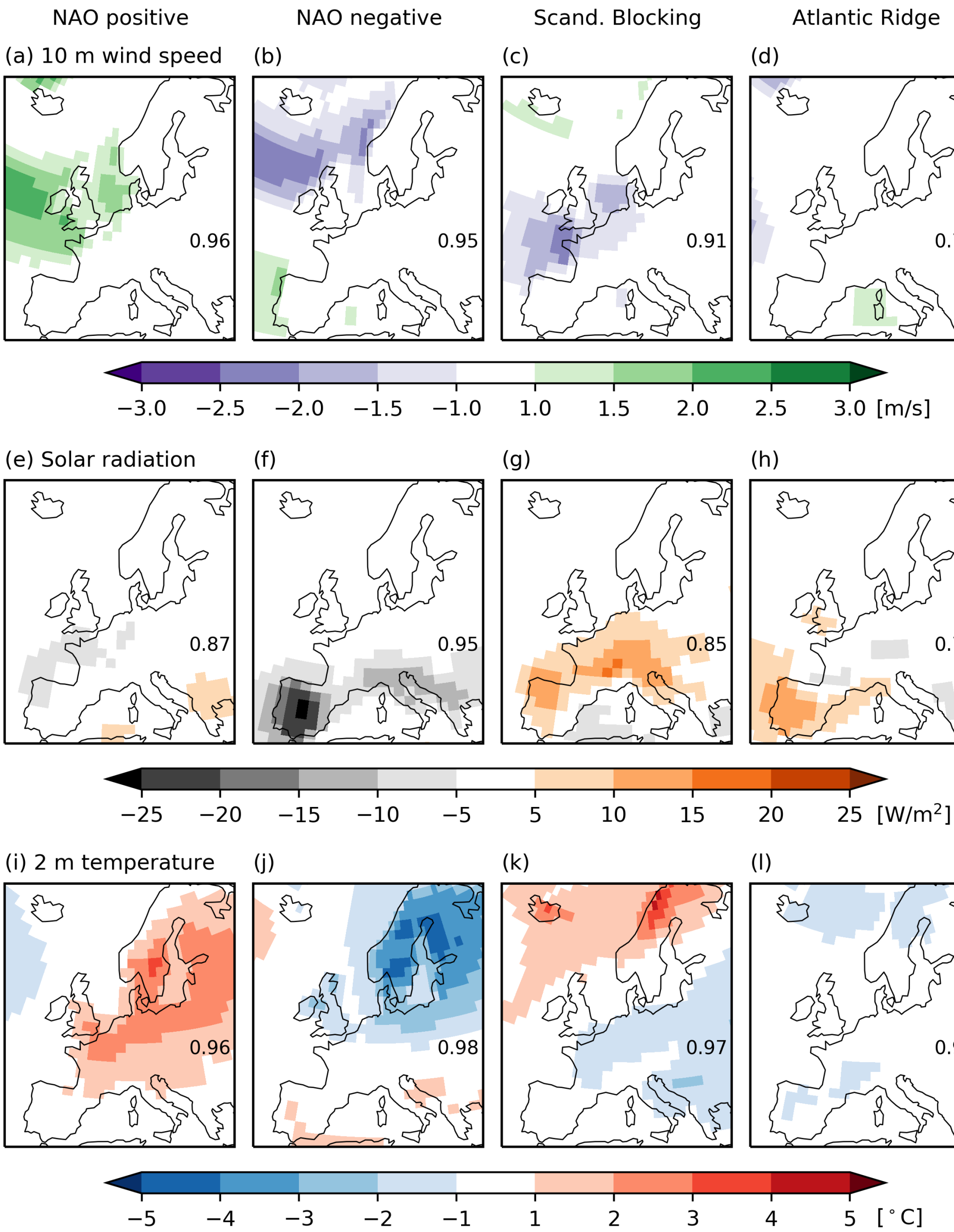

Figure S3. As Figure 2 of the main text, but here based on simulated data from the HadGEM2-ES model. Values denote the pattern correlation coefficient between the map shown and that based on ERA5 data.

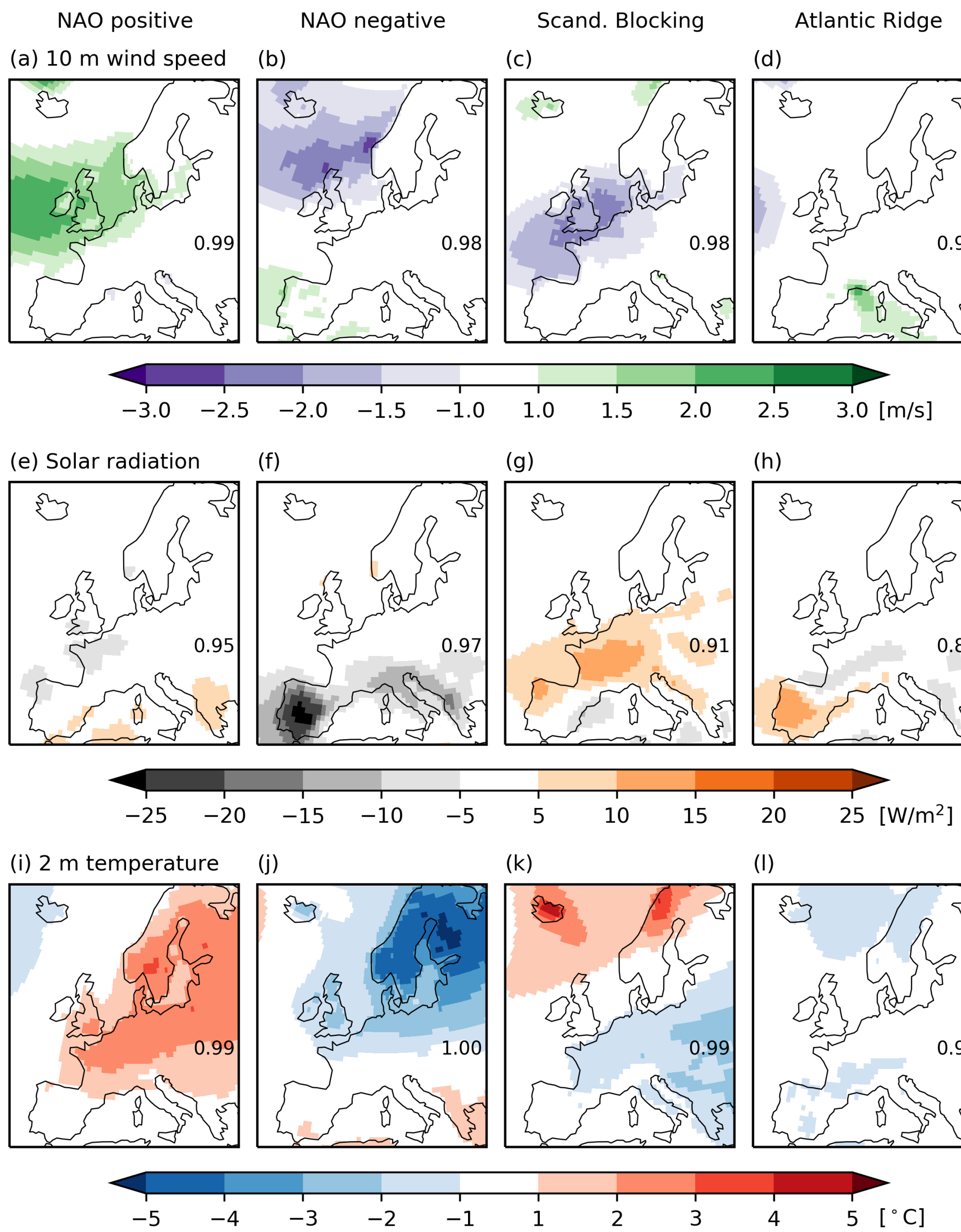

Figure S4. As Figure 2 of the main text, but here based on data from the ERA-Interim reanalysis product. Values denote the pattern correlation coefficient between the map shown and that based on ERA5 data.

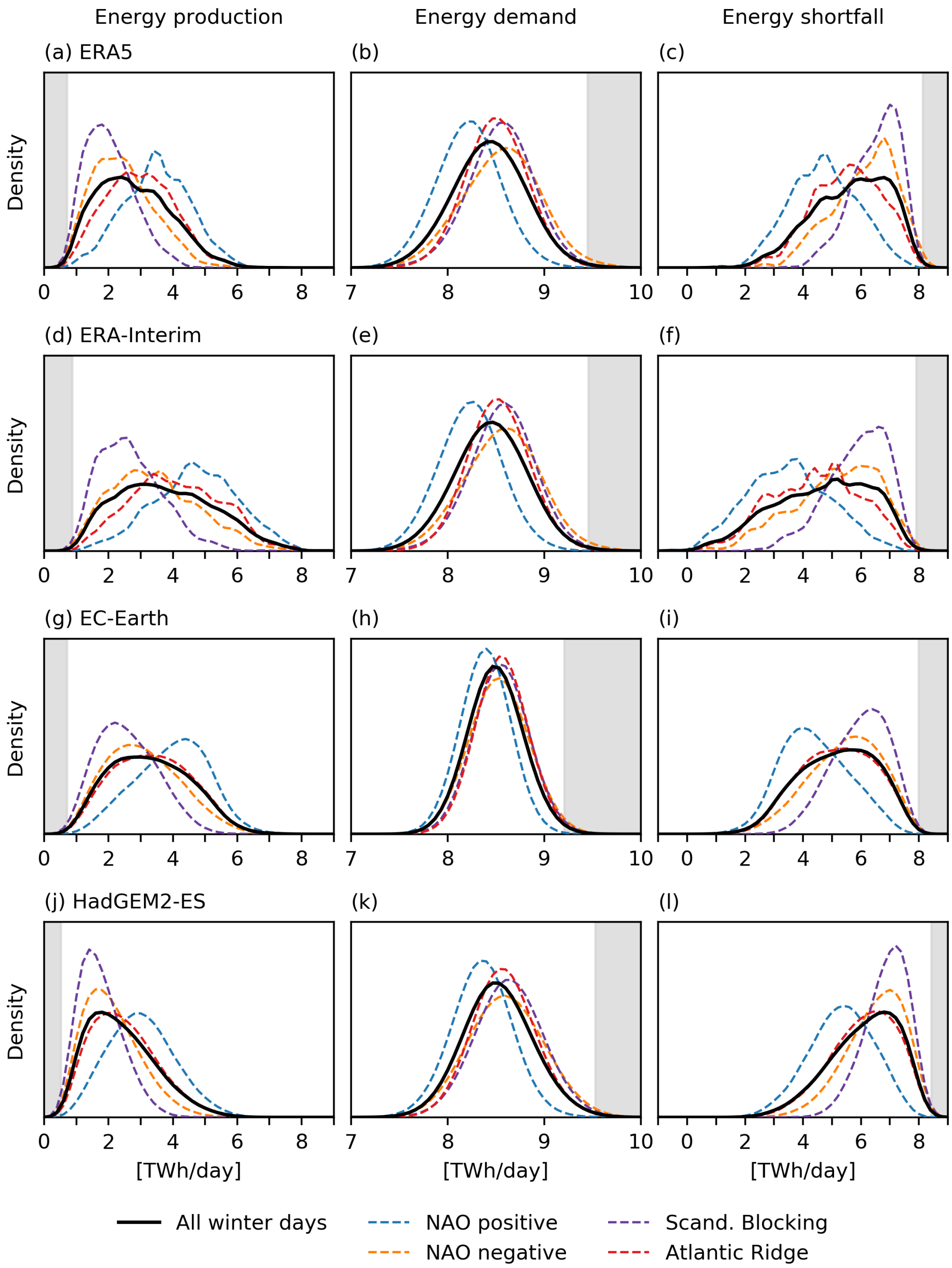

Figure S5. (a-c) Reproduction of Figure 4d-f of the main text. The other panels show the same but for ERA-interim and GCM data, (d-f) ERA-interim data, (g-i) EC-Earth simulated data, (j-l) HadGEM2-ES simulated data.

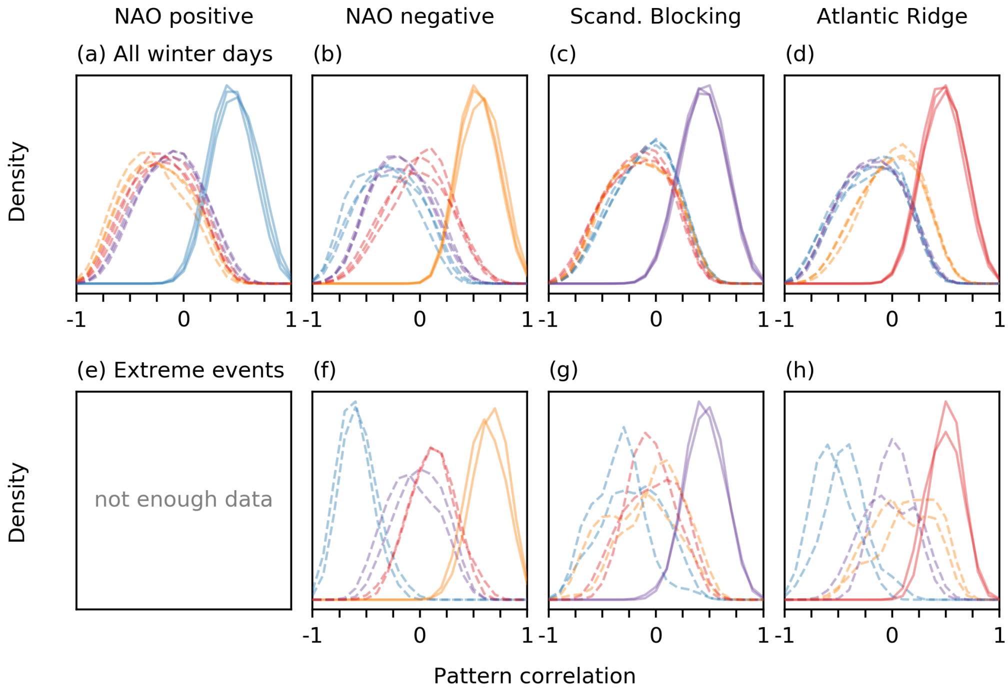

Figure S6. Distributions of pattern correlations for days assigned to a cluster and the cluster centroids. Pattern correlations determined based on 500 hPa geopotential height anomalies in North Atlantic-European region (90°W-30°E, 20°-80°N). (a-d) For all days classified in a regime, (e-h) for 1-in-10 year extreme high energy shortfall events classified in a regime. Colours as in Figure S5, bold lines show ERA5 data (only a-d, i-l), lighter lines show large ensemble simulated data. Solid lines show correlations/projections compared to the regime centroid, dashed lines show the correlations/projections compared to the other three regime centroids.

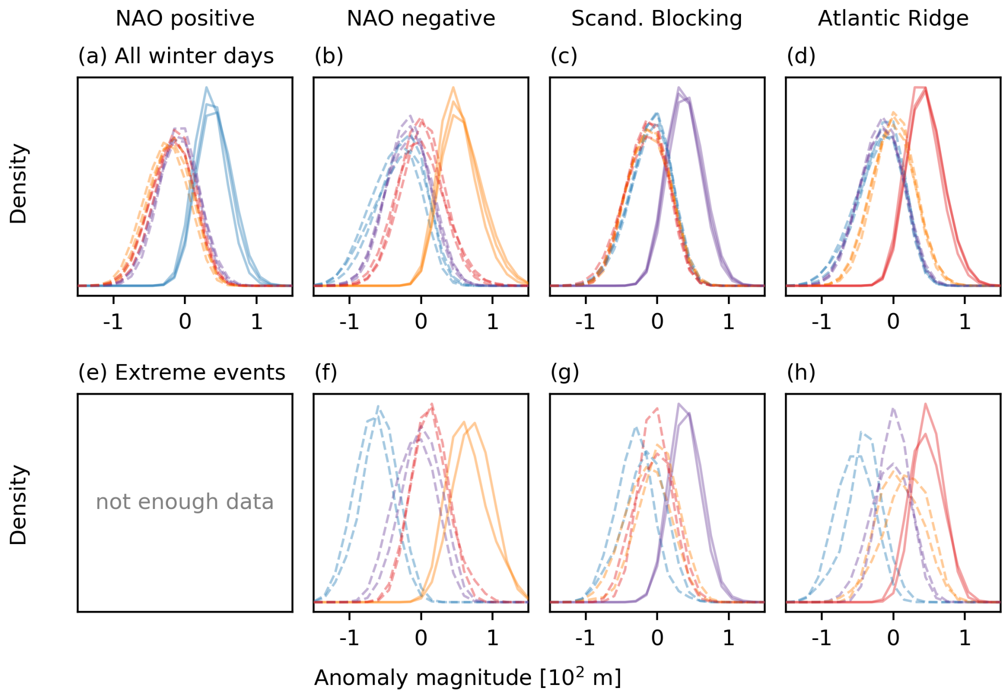

Figure S7. As Figure S6, but here for distributions of anomaly magnitudes [10^2 m] for days assigned to a cluster and the cluster centroids. Anomaly magnitudes determined by means of a projection of 500 hPa geopotential height anomalies in North Atlantic-European region (90°W-30°E, 20°-80°N) onto the regime centroid.

Table S1. Mean of the distribution of energy production/demand/shortfall in the full winter and separated by weather regime (TWh day^{-1}).

	winter	**NAO+**	**NAO-**	**Sc.Bl.**	**Atl.Ri.**
Energy production [TWh day^{-1}]					
ERA5	2.8	3.5	2.4	2.0	3.0
EC-Earth	3.3	4.0	3.1	2.6	3.4
HadGEM2-ES	2.4	3.0	2.1	1.8	2.5
Energy demand [TWh day^{-1}]					
ERA5	8.4	8.2	8.6	8.6	8.5
EC-Earth	8.5	8.4	8.5	8.6	8.6
HadGEM2-ES	8.5	8.4	8.6	8.6	8.6
Energy shortfall [TWh day^{-1}]					
ERA5	5.6	4.7	6.1	6.5	5.5
EC-Earth	5.2	4.4	5.4	6.0	5.2
HadGEM2-ES	6.1	5.3	6.5	6.9	6.1

Table S2. Standard deviation of the distribution of energy production/demand/shortfall in the full winter and separated by weather regime (TWh day^{-1}).

	winter	**NAO+**	**NAO-**	**Sc.Bl.**	**Atl.Ri.**
Energy production [TWh day^{-1}]					
ERA5	1.1	1.0	0.9	0.7	1.0
EC-Earth	1.2	1.1	1.2	0.9	1.2
HadGEM2-ES	1.0	1.0	0.9	0.7	1.0
Energy demand [TWh day^{-1}]					
ERA5	0.3	0.3	0.4	0.3	0.3
EC-Earth	0.2	0.2	0.2	0.2	0.2
HadGEM2-ES	0.3	0.2	0.3	0.3	0.3
Energy shortfall [TWh day^{-1}]					
ERA5	1.3	1.2	1.1	0.8	1.2
EC-Earth	1.3	1.2	1.3	1.0	1.3
HadGEM2-ES	1.2	1.1	1.0	0.7	1.1

Table S3. Skewness of the distribution of energy production/demand/shortfall in the full winter and separated by weather regime (no units). Asterisks indicate when skewness is significantly different from 0 at $\alpha = 0.05$.

	winter	**NAO+**	**NAO-**	**Sc.Bl.**	**Atl.Ri.**
Energy production [no units]					
ERA5	0.42*	0.04	0.53*	0.61*	0.26*
EC-Earth	0.24*	−0.15*	0.41*	0.41*	0.17*
HadGEM2-ES	0.64*	0.27*	0.72*	0.69*	0.57*
Energy demand [no units]					
ERA5	−0.00	0.03	−0.08	−0.20	−0.00
EC-Earth	0.16*	−0.10*	0.09*	0.11*	0.10*
HadGEM2-ES	0.20*	0.03*	0.07*	0.04*	0.26*
Energy shortfall [no units]					
ERA5	−0.44	−0.02	−0.60*	−0.63*	−0.27*
EC-Earth	−0.23*	0.17*	−0.40*	− 0.41*	−0.15*
HadGEM2-ES	−0.54*	−0.20*	−0.62*	−0.58*	−0.48*

Table S4. Risk ratios of energy production/demand/shortfall extremes in the full winter and separated by weather regime (no units). Asterisks indicate when the risk ratio is significantly different from 1.00 at $\alpha = 0.05$, determined by a $N = 10,000$ bootstrapping exercise.

	winter	**NAO+**	**NAO-**	**Sc.Bl.**	**Atl.Ri.**
Energy production [no units]					
ERA5	1.00	0.00*	2.56	1.81	0.00*
EC-Earth	1.00	0.08*	1.13	2.26*	0.70*
HadGEM2-ES	1.00	0.14*	1.51*	2.17*	0.51*
Energy demand [no units]					
ERA5	1.00	0.00*	5.11*	0.00*	0.00*
EC-Earth	1.00	0.00*	1.98*	1.47*	1.03
HadGEM2-ES	1.00	0.00*	2.54*	1.37*	0.75
Energy shortfall [no units]					
ERA5	1.00	0.00*	3.84	0.91	0.00
EC-Earth	1.00	0.02*	1.85*	1.40*	1.21
HadGEM2-ES	1.00	0.03*	2.12*	1.62*	1.77*